Proceedings of GT2005
ASME Turbo Expo 2005: Power for Land, Sea and Air
June 6-9, 2005, Reno-Tahoe, Nevada, USA

GT2005-68600

Effect of Reynolds Number and Periodic Unsteady Wake Flow Condition on Boundary Layer Development, Separation, and Re-attachment along the Suction Surface of a Low Pressure Turbine Blade

B. Öztürk, M. T. Schobeiri,
Turbomachinery Performance and Flow Research Laboratory
Texas A&M University
College Station, Texas

David E. Ashpis
National Aeronautics and Space Administration
John H. Glenn Research Center at Lewis Field
Cleveland, OH 44135-3191

ABSTRACT

The paper experimentally studies the effects of periodic unsteady wake flow and different Reynolds numbers on boundary layer development, separation and re-attachment along the suction surface of a low pressure turbine blade. The experimental investigations were performed on a large scale, subsonic unsteady turbine cascade research facility at Turbomachinery Performance and Flow Research Laboratory (TPFL) of Texas A&M University. The experiments were carried out at Reynolds numbers of 110,000 and 150,000 (based on suction surface length and exit velocity). One steady and two different unsteady inlet flow conditions with the corresponding passing frequencies, wake velocities, and turbulence intensities were investigated. The reduced frequencies chosen cover the operating range of LP turbines. In addition to the unsteady boundary layer measurements, surface pressure measurements were performed. The inception, onset, and the extent of the separation bubble information collected from the pressure measurements were compared with the hot wire measurements.

The results presented in ensemble-averaged, and the contour plot forms help to understand the physics of the separation phenomenon under periodic unsteady wake flow and different Reynolds number. It was found that the suction surface displayed a strong separation bubble for these three different reduced frequencies. For each condition, the locations defining the separation bubble were determined carefully analyzing and examining the pressure and mean velocity profile data. The location of the boundary layer separation was dependent of the Reynolds number. It is observed that starting point of the separation bubble and the re-attachment point move further downstream by increasing Reynolds number from 110,000 to 150,000. Also, the size of the separation bubble is smaller when compared to that for Re=110,000.

NOMENCLATURE

c	blade chord
c_{ax}	axial chord
C_p	pressure coefficient, $C_p = \frac{p_i - p_s}{(p_t - p_s)_{inl}}$
d_R	rod diameter
H_{12}	shape factor, $H_{12}=\delta_1/\delta_2$
h_m	maximum separation bubble height
L_{SS}	suction surface length
M	number of samples
N	number of wake cycles
p_i	static pressure taps i=1,..,48
p_s, p_t	static and total pressure at the inlet
Re_{LSS}	Reynolds number based $Re = L_{ss}V_{exit}/\nu$
S_B	blade spacing
S_R	rod spacing
s	streamwise distance from the leading edge of the blade
s_o	streamwise distance from the leading edge to the trailing edge of the blade
s_{md}	maximum separation bubble height at a

	streamwise distance from blade leading edge
s_r	re-attachment point of the separation bubble at a streamwise distance from blade leading edge
s_s	starting point of the separation bubble at a streamwise distance from blade leading edge
t	time
Tu	turbulence intensity
U	belt translational velocity
V_{ax}	axial velocity
V_{exit}	exit velocity
V	velocity
v	fluctuation velocity
γ	blades stagger angle
δ	boundary layer thickness
δ_1	boundary layer displacement thickness
δ_2	boundary layer momentum thickness
δ_3	boundary layer energy thickness
ν	kinematic viscosity
σ	cascade solidity, $\sigma = c/S_B$
τ	one wake-passing period
φ	flow coefficient, $\varphi = V_{ax}/U$
ψ_A	Zweifel coefficient $\psi_A = 2\sin^2\alpha_2\left(\cot\alpha_2 - \cot\alpha_1\right)s_B/c_{ax}$
Ω	reduced frequency $\Omega = \frac{c}{S_R}\frac{U}{V_{ax}} = \frac{\sigma}{\varphi}\frac{S_B}{S_R}$

INTRODUCTION

In recent years, gas turbine engine aerodynamicists have focused their attention on improving the efficiency and performance of the low pressure turbine (LPT) component. Research works from industry, research centers, and academia have shown that a reduction of the blade number can be achieved without substantially sacrificing the efficiency of the LPT blading. This reduction contributes to an increase in thrust/weight ratio, thus reducing the fuel consumption. Contrary to the high pressure turbine (HPT) stage group that operates in a relatively high Reynolds number environment, dependent on operation conditions, the LPT experiences a variation in Reynolds number ranging from 50,000 to 250,000. Since the major portion of the boundary layer, particularly along the suction surface is laminar, the low Reynolds number in conjunction with the local adverse pressure gradient makes it susceptible to flow separation, thus increasing the complexity of the LPT boundary layer aerodynamics. The periodic unsteady nature of the incoming flow associated with wakes that originate from upstream blades substantially influences the boundary layer development including the onset of the laminar separation, the extent of the separation bubble, and its turbulent re-attachment. Of particular relevance in the context of LPT aerodynamics is the interaction of the wake flow with the suction surface separation bubble. While the phenomenon of the unsteady boundary layer development and transition in the absence of the separation bubbles has been the subject of intensive research, that has led to better understanding the transition phenomenon, comprehending the multiple effects of mutually interacting parameters on the LPT boundary layer separation and their physics still requires more research.

The significance of the unsteady flow effect on efficiency and performance of compressor and turbine stages was recognized in the early seventies by several researchers. Fundamental studies by Pfeil and Herbst [1], Pfeil et al. [2], and Orth [3] studied and quantified the effect of unsteady wake flow on the boundary layer transition along flat plates. Schobeiri and his co-workers [4], [5], [6], [7] experimentally investigated the effects of the periodic unsteady wake flow and pressure gradient on the boundary layer transition and heat transfer along the concave surface of a constant curvature plate. The measurements were systematically performed under different pressure gradients and unsteady wake frequencies using a squirrel cage type wake generator positioned upstream of the curved plate. Liu and Rodi [8] carried out the boundary layer and heat transfer measurements on a turbine cascade, which was installed downstream of a squirrel cage type wake generator mentioned previously.

Analyzing the velocity and the turbulence structure of the impinging wakes and their interaction with the boundary layer along the concave side of the curved plate, Chakka and Schobeiri [7] developed an intermittency based unsteady boundary layer transition model. The analysis revealed a universal pattern for the relative intermittency function for all the frequencies and pressure gradients investigated. However, the curved plate investigations were not sufficient to draw any conclusion with regard to an eventual universal character of the relative intermittency function. Further detailed investigations of the unsteady boundary layer on a high Reynolds number turbine cascade by Schobeiri et al. [9], [10] and its subsequent analysis [11] and [12] verified the universal character of the relative intermittency function. For this purpose, Schobeiri et al. [9] utilized a conceptually different type wake generator, which is also used for the investigation presented in this paper. Fottner and his coworkers [13], [14] and Schulte and Hodson [15] used the same wake generating concept for the investigations on the influence of the unsteady wake flow on the LPT-

boundary layer. Kaszeta, Simon, and Ashpis [16] experimentally investigated the laminar-turbulent transition aspect within a channel with the side walls resembling the suction and pressure surfaces of a LPT blade. Lou and Hourmouziadis [17] investigated the mechanism of separation, transition, and re-attachment, and the effect of oscillating inlet flow conditions on laminar boundary layer separation along a flat plate under a strong negative pressure gradient which was similar to the LPT pressure gradient. This was simulated by contouring the top wall. They studied the Reynolds number effect on the transition region. Their results showed that the higher Reynolds numbers cause an earlier transition and reduction of the transition length, while the separation point does not change its location. Using the top wall contouring, Volino and Hultgren [18] performed an experimental study and measured the detailed velocity along a flat plate which was subjected to a similar pressure gradient as the suction side of a low pressure turbine blade. They also stated that the location of the boundary layer separation does not strongly depend on the Reynolds number or free-stream turbulence level, as long as the boundary layer remains non-turbulent before separation occurs. Furthermore, they showed that the extent of the transition is strongly dependent on the Reynolds number and turbulence intensity.

Using the surface mounted hot film measurement technique, Fottner and his coworkers [13] and [14], Schröder [19], and Haueisen, Hennecke, and Schröder [20] documented strong interaction between the wakes and the suction surface separation bubble on the LPT blades, both in the wind tunnel cascade tests and in a turbine rig. Furthermore, they investigated the boundary layer transition under the influence of the periodic wakes along the LPT surface and found that the interaction of the wake with the boundary layer greatly affects the loss generation. Shyne et al. [21] performed an experimental study on a simulated low pressure turbine. The experiments were carried out at Reynolds numbers of 100,000 and 250,000 with three levels of free-stream turbulence. They indicated that the transition onset and the length are strongly dependent on the free-stream turbulence. As the free-stream turbulence increases, the onset location and the length of the transition are decreased. Treuren et al. [22] performed an experimental study along a LPT surface at the very low Reynolds number of 25,000 and 50,000 with different free-stream turbulence levels. They showed that a massive separation at the very low Reynolds number of 25,000 is persistent, in spite of an elevated free stream turbulence intensity. However, at the higher Reynolds number of 50,000, there was a strong separation on the suction side for the low free-stream turbulence level. The separation bubble was eliminated for the higher free-stream turbulence level of 8-9%. The investigations by Halstead et al. [23] on a large scale LP turbine uses surface mounted hot films to acquire detailed information about the quasi-shear stress directly on the blade surface. Investigations by Cardamone et al. [14] and Schröder [19] indicate that the benefit of the wake-boundary layer interaction can be used for the design procedure of modern gas turbine engines with a reduced LPT blade number without altering the stage efficiency.

Most of the studies mentioned above on LP turbine cascade aerodynamics have largely concentrated on the measurement of the signals stemming from hot films mounted on the suction and pressure surfaces of the blades under investigation. Although this technique is qualitatively reflecting the interaction of the unsteady wake with the boundary layer, because of the lack of an appropriate calibration method, it is not capable of quantifying the surface properties such as the wall shear stress. The few boundary layer measurements are not comprehensive enough to provide any conclusive evidence for interpretation of the boundary layer transition and separation processes and their direct impact on profile loss, which is a critical parameter for blade design. Furthermore, the numerical simulation of the unsteady LPT blade aerodynamics using conventional turbulence and transition models fails if it is applied to low Reynolds number cases. Recent work presented by Cardamone et al. [14] shows that in the steady state case at Re= 60,000, the separation is captured, however, for the unsteady case, the separation bubble is not reproduced.

A recent experimental study by Schobeiri and Öztürk [24],[25] investigated the physics of the inception, onset and extent of the separation bubble along a low pressure turbine blade which was the first part of a series of investigations carried out at TPFL. A detailed experimental study on the behavior of the separation bubble on the suction surface of a highly loaded LPT blade under a periodic unsteady wake flow was presented in [24]. Surface pressure measurements were performed at Re= 50,000, 75,000, 100,000, 125,000. Increasing the Reynolds number has resulted in no major changes to the surface pressure distribution. They concluded that the unsteady wake flow with its highly turbulent vortical core over the separation region caused a periodic contraction and expansion of the separation bubble. It was proposed that, in conjunction with the pressure gradient and periodic wakes, the

temporal gradient of the turbulence fluctuation, or more precisely the fluctuation acceleration $\partial v_{rms}/\partial t$ provides a higher momentum and energy transfer into the boundary layer, energizing the separation bubble and causing it to partially or entirely disappear. They found that for $\partial v_{rms}/\partial t > 0$, the separation bubble starts to contract whereas for $\partial v_{rms}/\partial t < 0$, it gradually assumes the shape before the contraction. They argued that not only the existence of higher turbulence fluctuations expressed in terms of higher turbulence intensity influences the flow separation, but also its gradient is of crucial importance in suppressing or preventing the onset and the extent of the separation bubble. They stated that the fluctuation gradient is an inherent feature of the incoming periodic wake flow and does not exist in a statistically steady flow that might have a high turbulence intensity. They also stated that, unsteady wake flow with its highly turbulent vortical core over the separation region, caused a periodic contraction and extension of the separation bubble and a reduction of the separation bubble height. Increasing the passing frequency associated with a higher turbulence intensity further reduced the separation bubble height [25].

The objective of the present study dealing with the specific issues of the LPT boundary layer aerodynamics is to provide a detailed unsteady boundary flow information to understand the underlying physics of the inception, onset, and extension of the separation bubble for different Reynolds numbers. Furthermore, the unsteady boundary layer data from the present and planned experimental investigations will serve to extend the intermittency unsteady boundary layer transition model developed by Schobeiri and his coworkers [7, 11, 12] to the LPT cases, where a massive separation occurs on the suction surface at a low Reynolds number at the design and off-design incidence. Furthermore, the experimental results are intended to serve as benchmark data for a comparison with numerical computation using DNS or RANS-codes.

It is well known that the boundary layer measurement is one of the most time consuming aerodynamic measurements. Any attempt to increase the number of parameters to be studied would inevitably result in substantial increase of the measurement time. Considering this fact, the research facility described in [9] and [10] with state-of-the-art instrumentation has been substantially modified to study systematically and efficiently the influence of the periodic unsteady and highly turbulent flow on the LPT cascade aerodynamics at the design and off-design incidence angles, where the Reynolds number, wake impingement frequency, free-stream turbulence, and the blade solidity can be varied independently.

EXPERIMENTAL RESEARCH FACILITY

To investigate the effect of unsteady wake flow on turbine and compressor cascade aerodynamics, particularly on unsteady boundary layer transition, a multi-purpose large-scale, subsonic research facility was designed and has been taken into operation since 1993. Since the facility in its original configuration is described in [9], [10] and [24] only a brief description of the modifications and the main components is given below. The research facility consists of a large centrifugal compressor, a diffuser, a settling chamber, a nozzle, an unsteady wake generator, and a turbine cascade test section as shown in Figure 1. The compressor with a volumetric flow rate of 15 m^3/s is capable of generating a maximum mean velocity of 100 m/s at the test section inlet. The settling chamber consists of five screens and one honeycomb flow straightener to control the uniformity of the flow.

Two-dimensional periodic unsteady inlet flow is simulated by the translational motion of an unsteady wake generator (see Figure 2), with a series of cylindrical rods attached to two parallel operating timing belts driven by an electric motor. To simulate the wake width and spacing that stem from the trailing edge of rotor blades, the diameter and number of rods can be varied. The rod diameter, its distance from the LPT blade leading edge, the wake width and the corresponding drag coefficient is chosen according to the criteria outlined by Schobeiri et al. [26]. The belt-pulley system is driven by an electric motor and a frequency controller. The wake-passing frequency is monitored by a fiber-optic sensor. The sensor also serves as the triggering mechanism for data transfer and its initialization, which is required for ensemble-averaging. This type of wake generator produces clean 2-dimensional wakes, whose turbulence structure, decay and development is, to a great extent, predictable [26]. The unsteady boundary layer transition and heat transfer investigations [9-12] performed on this facility serve as the bench mark data for validation of turbulence models, transition models, and general code assessments.

To account for a high flow deflection of the LPT cascade, the entire wake generator and test section unit including the traversing system, was modified to allow a precise angle adjustment of the cascade relative to the incoming flow. This is done by a hydraulic platform, which simultaneously lifts and rotates the wake generator and test section unit. The unit is then attached

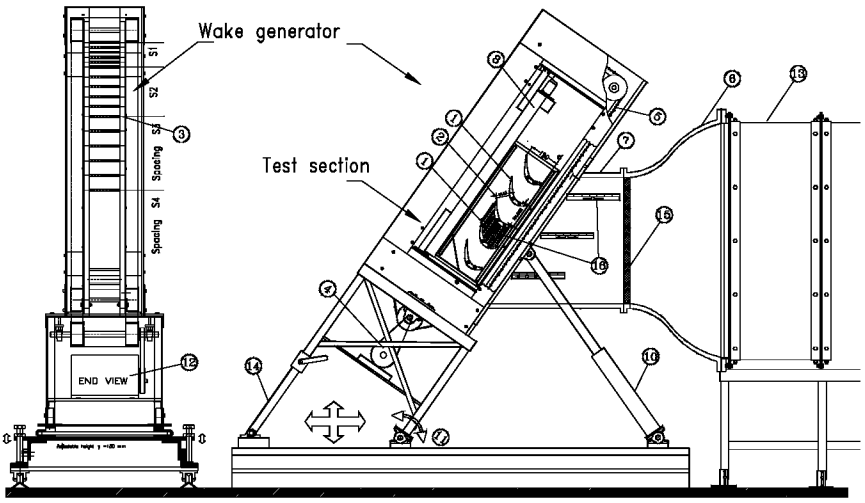

① Static pressure blade
② Blade with hot film sensors
③ Wake generating rods
④ Wake generator
⑤ Timing belts. rod attachments
⑥ Transition duct
⑦ Straight duct
⑧ Traversing system
⑨ Inlet nozzle
⑩ Hydraulic cylinders
⑪ Pivot point
⑫ Wake generator e-motor
⑬ Large silence chamber with honeycom and five screens
⑭ Telescope supprt
⑮ Honeycomb flow straightener
⑯ Traversing slots

Figure 1. Turbine cascade research facility with the components and the adjustable test section

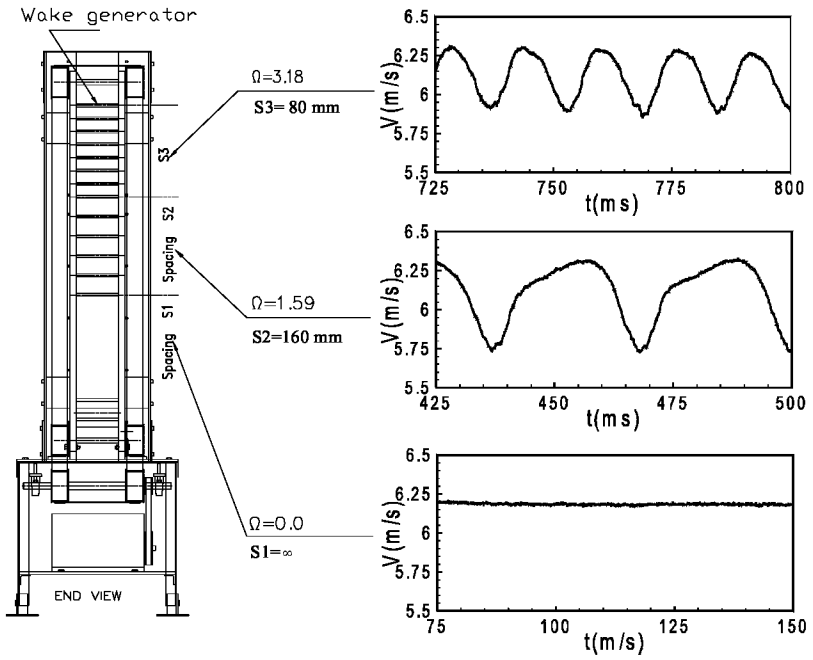

Figure 2. Wake Generator

Table 1: Parameters of turbine cascade test section

Parameters	Values	Parameters	Values
Inlet velocity	V_{in} = 4 m/s	Inlet turbulence intensity	Tu_{in} = 1.9 %
Rod translational speed	U = 5.0 m/s	Blade Re-number	Re = 110,000
Nozzle width	W = 200.0 mm	Blade height	h_B = 200 mm
Blade chord	c = 203.44 mm	Cascade solidity	$\sigma = 1.248$
Blade axial chord	c_{ax} = 182.85mm	Zweifel coefficient	ψ_A = 1.254
Blade suction surface length	L_{SS} = 270.32 mm	Cascade angle	$\varphi = 55°$
Cascade flow coefficient	Φ = 0.80	Cascade spacing	S_B = 163 mm
Inlet air angle to the cascade	$\alpha_1 = 0°$	Exit air angle from the cascade	$\alpha_2 = 90°$
Rod diameter	D_R = 2.0 mm	Rod distance to lead. edge	L_R = 122 mm
Cluster 1 (no rod, steady)	$S_R = \infty$ mm	Ω - parameter steady case	Ω = 0.0
Cluster 2 rod spacing	S_R = 160.0 mm	Ω - parameter for cluster 1	Ω = 1.59
Cluster 3 rod spacing	S_R = 80.0 mm	Ω - parameter for cluster 2	Ω = 3.18

to the tunnel exit nozzle with an angular accuracy less than 0.05°, which is measured electronically.

The special design of the facility and the length of the belts (L_{belt} = 4,960 mm) enables a considerable reduction of the measurement time. For the present investigation, two clusters of rods with constant diameter of 2 mm are attached to the belts as shown in Figure 2. The two clusters with spacings S_R = 160 mm and S_R = 80 mm are separated by a distance which does not have any rods, thus simulating steady state case ($S_R = \infty$). Thus, it is possible to measure sequentially the effect of three different spacings at a single boundary layer point. To clearly define the influence domain of each individual cluster with the other one, the clusters are arranged with a certain distance between each other. Using the triggering system mentioned above and a continuous data acquisition, the buffer zones between the data clusters can be readily identified.

The data analysis program cuts the buffer zones and evaluates the data pertaining to each cluster. Comprehensive preliminary measurements were carried out to make sure that the data were exactly identical to those, when the entire belt length was attached with rods of constant spacing, which corresponded to each individual cluster spacing. The cascade test section shown in Figure 1, located downstream of the wake generator, includes 5 LPT blades with a height of 200.0 mm and the chord of 203.44 mm. For boundary layer investigations, five identical "Pak B" airfoils designed by Pratt & Whitney were implemented whose cascade geometry is given in Table 1.

The blade geometry resembles the essential feature such as the laminar boundary layer separation that is inherent to typical LPT blades. The blade geometry was made available to NASA researchers and academia to study the specific problems of LPT flow separation, its passive and active control and its prevention. As shown in [9], this blade number is necessary and sufficient to secure a spatial periodicity for the cascade flow. The periodicity is noticed in the pressure distribution for the second and fourth blade for steady and unsteady flow conditions, and is shown in Figure 1. These blades were specially manufactured for measurement of pressure and showed identical pressure distributions.

A computer controlled traversing system is used to measure the inlet velocities and turbulence intensities, as well as the boundary layers on suction and pressure surfaces. The traversing system (see Figure 3) was

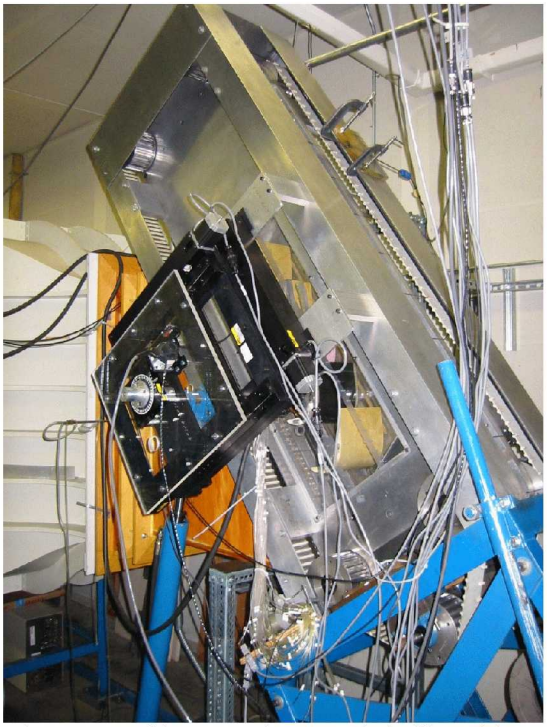

Figure 3. Turbine cascade research facility with 3-axis traversing system

modified to allow the probe to reach all streamwise positions along the suction und pressure surfaces. The three axis traversing system is vertically mounted on the plexiglass side wall. Each axis is connected to a DC-stepper motor with an encoder and decoder. The optical encoder provides a continuous feedback to the stepper motor for accurate positioning of the probes. The system is capable of traversing along the suction and pressure surfaces in small steps up to 1 μm, and the third axis is capable of rotating with an angular accuracy less then 0.05°, which is specifically required for boundary layer investigations where the measurement of the laminar sublayer is of particular interest.

INSTRUMENTATION, DATA ACQUISITION, AND DATA REDUCTION

The data acquisition system is controlled by a personal computer that includes a 16 channel, 12-bit analog-digital (A/D) board. Time dependent velocity signals are obtained by using a commercial 3-channel (TSI), constant temperature hot-wire anemometer system that has a signal conditioner with a variable low pass filter and adjustable gain. A Prandtl probe, placed upstream of the diffuser, monitors the reference velocity at a fixed location. The pneumatic probes are connected to high precision differential pressure transducers for digital readout. Several calibrated thermocouples are placed downstream of the test section to constantly monitor the flow temperature. The wake generator speed and the passing frequency signals of the rods are transmitted by a fiber-optic trigger sensor. The passage signals of the rods are detected by the sensor using a silver-coated reflective paint on one of the belts. This sensor gives an accurate readout of the speed of the wake generator and the passing frequency of the rods. The signals of the pressure transducers, thermocouples, and trigger sensors are transmitted to the A/D board and are sampled by the computer. To ensure the cascade periodicity, the second and fourth blades are instrumented each with 48 static pressure taps. Two adjacent blades are used for boundary layer measurement. The taps are connected to a scanivalve, which sequentially transferred the pressure signals to one of the transducers that was connected to the A/D board.

The unsteady data are taken by calibrated, custom designed miniature, single hot wire probes. At each boundary layer position, samples were taken at a rate of 20kHz for each of 100 revolutions of the wake generator. The data were ensemble-averaged with respect to the rotational period of the wake generator. Before final data were taken, the number of samples per revolution and the total number of revolutions were varied to determine the optimum settings for convergence of the ensemble-average.

For the steady state case, the instantaneous velocity components are calculated from the temperature compensated instantaneous voltages by using the calibration coefficients. The instantaneous velocity can be represented in the following form:

$$V = \bar{V} + v \tag{1}$$

where $\bar{V}$ is the mean (time-averaged) velocity and v is the turbulent fluctuation component. The mean velocity, also known as the time-average, is given by:

$$\bar{V} = \frac{1}{M}\sum_{j=1}^{M} V_j \tag{2}$$

where M is the total number of samples at one boundary

layer location. The root mean square value of the turbulent velocity fluctuation is:

$$v = \sqrt{\frac{1}{M}\sum_{j=1}^{M}(V_j - \bar{V})^2} \quad (3)$$

and the local turbulence intensity is defined as:

$$Tu_{loc} = \frac{v}{\bar{V}} \times 100 = \frac{1}{\bar{V}}\sqrt{\frac{1}{M}\sum_{j=1}^{M}(V_j - \bar{V})^2} \times 100 \quad (4)$$

For unsteady cases, the ensemble-averaged velocity, fluctuation velocity, and the turbulence intensity were calculated from the instantaneous velocity samples by:

$$V_i(t_i) \equiv \langle V_i(t_i)\rangle = \frac{1}{N}\sum_{j=1}^{N} V_{ij}(t_i) \quad (5)$$

$$v_i(t_i) \equiv \langle v_i(t_i)\rangle = \sqrt{\frac{1}{N}\sum_{j=1}^{N}\left[V_{ij}(t_i) - \langle V_i(t_i)\rangle\right]^2} \quad (6)$$

$$Tu_i(t_i)\rangle \equiv \langle Tu_i(t_i)\rangle = \frac{\langle v_i(t_i)\rangle}{\langle V_i(t_i)\rangle} \times 100 \quad (7)$$

where N= 100 is the total number of wake generator periods and M the number of samples taken per period. $\langle V_i(t_i)\rangle$ is the reference ensemble averaged velocity for the particular boundary layer traverse.

EXPERIMENTAL RESULTS AND DISCUSSION

To investigate the influence of the unsteady wake flow on the boundary layer development along the suction and pressure surfaces of the LPT blade and, particularly, its impact on the inception and onset of the separation bubble, the detailed surface pressure and boundary layer measurements were performed at a Reynolds number of 110,000 and 150,000. This Reynolds numbers, which pertain to a typical cruise operation , exhibit a representative value within LPT operating range between 75,000 and 400,000 as discussed by Hourmouziadis [27]. Furthermore, it produces separation bubbles that can be accurately measured by miniature hot wire probes. For the Reynolds number of 110,000 and 150,000, three different reduced frequencies were examined. For generation of the unsteady wakes, cylindrical rods with the diameter d_R = 2mm were chosen to fulfill the criterion that requires the generation of a drag coefficient C_D that is approximately equal to the C_D of the turbine blade with the chord and spacing given in Table 1 (for details look for the studies in [26] and [28]).

To accurately account for the unsteadiness caused by the frequency of the individual wakes and their spacings, the flow velocity, and the cascade parameters, a reduced frequency Ω is defined that includes the cascade solidity σ, the flow coefficient φ, the blade spacing S_B, and the rod spacing S_R. Many researchers have used Strouhal number as the unsteady flow parameter, which only includes the speed of the wake generator and the inlet velocity. However, the currently defined reduced frequency Ω is an extension of Strouhal number in the sense that it incorporates the rod spacing S_R and the blade spacing S_B in addition to the inlet velocity and wake generator speed. For surface pressure measurement rods with uniform spacings as specified in Table 1 were attached over the entire belt length. For boundary layer measurement, however, clusters of rods were attached, as mentioned previously.

Surface Pressure Distributions

Detailed pneumatic surface pressure measurements were taken at Re = 110,000, and 150,000. For each Reynolds number three different reduced frequencies, namely Ω = 0.0, 1.59, and 3.18 are applied that correspond to the rod spacings S_R = 80 mm, 160 mm, and ∞ mm. The pressure distributions in Figure 4 show the results of the steady case and two unsteady cases. The pressure signals inherently signify the time-averaged pressure because of the internal pneumatic damping effect of the connecting pipes to the transducer. The noticeable deviation in pressure distribution between the steady and unsteady cases, especially on the suction surface, is due to the drag forces caused by the moving rods. The drag forces are imposed on the main stream and cause momentum deficiency that lead to a reduction of the total and static pressure.

The time-averaged pressure coefficients along the pressure and suction surfaces are plotted in Figure 4. The suction surface (upper portion), exhibits a strong negative pressure gradient. The flow accelerates at a relatively steep rate and reaches its maximum surface velocity that corresponds to the minimum C_p= -4.0 at s/s_o= 0.42. Passing through the minimum pressure, the fluid particles within the boundary layer encounter, a positive pressure gradient that causes a sharp

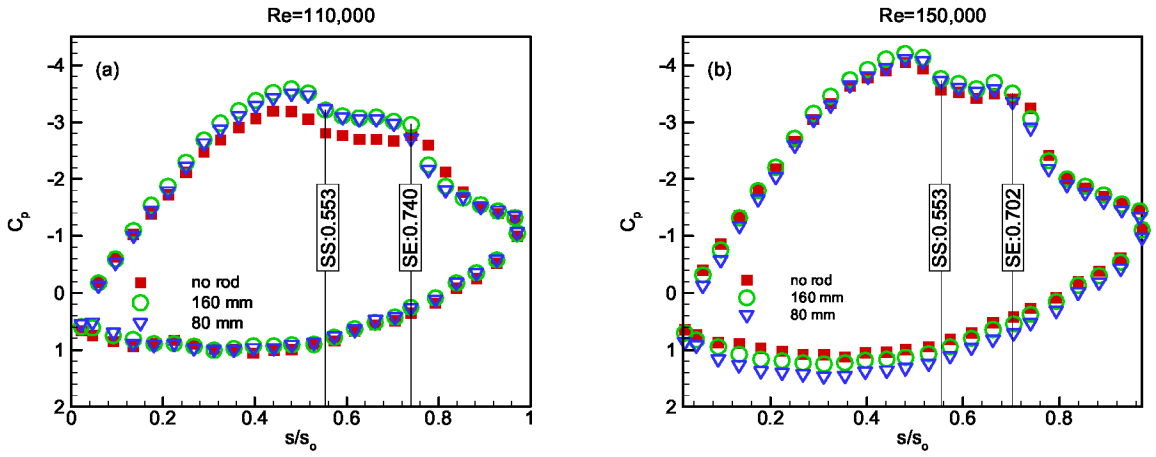

Figure 4. Static pressure distributions at two different Re-numbers and reduced frequencies Ω=0, 1.59, 3.18 (no rod, 160 mm, 80 mm), SS=Separation start, SE= Separation end

deceleration until s/s_o= 0.55 has been reached. This point signifies the beginning of the laminar boundary layer separation and the onset of a separation bubble. As seen in the subsequent boundary layer discussion, the separation bubble characterized by a constant C_p-plateau extends up to s/s_o= 0.746, thus occupying more than 19% of the suction surface and constituting a massive separation. Passing the plateau, the flow first experiences a second sharp deceleration indicative of a process of re-attachment followed by a further deceleration at a moderate rate. On the pressure surface, the flow accelerates at a very slow rate, reaches a minimum pressure coefficient at s/s_o= 0.42 and continues to accelerate until the trailing edge has been reached. Unlike the suction surface, the pressure surface boundary layer does not encounter any adverse positive pressure gradient that triggers separation. However, close to the leading edge, a small plateau extending from s/s_o= 0.08 to 0.16 indicates the existence of a small size separation bubble that might be attributed to a minor inlet flow incident angle.

Considering the unsteady case with the reduced frequency Ω = 1.59 corresponding to a rod spacing of S_R=160 mm, Figure 4 exhibits a slight difference in the pressure distribution between the steady and unsteady cases. As mentioned above, this deviation is attributed to the momentum deficiency that leads to a reduction of the total and static pressure. For Re=110,000, the wakes have a reducing impact on the streamwise extent of the separation plateau. As seen in Figure 4 (a), the trailing edge of the plateau has shifted from s/s_o= 0.74 to s/s_o= 0.702. This shift reduced the streamwise extent of the separation plateau from 19% to 15% of the suction surface length which is in this particular case, 21% of reduction in streamwise extent of the separation. Increasing the reduced frequency to Ω=3.18 by reducing the rod spacing to S_R=80 mm causes a slight shift of the C_p-distribution compared with Ω=1.59 case. One should bear in mind that pneumatically measured surface pressure distribution represents a time integral of the pressure events only.

Increasing the Reynolds number to Re=150,000, has brought major changes in steady state C_p-distribution. The combination of higher Re-number with unsteady wakes reveals the noticeable deviation on the streamwise extent of the separation plateau. As seen in Figure 4 (b), the trailing edge of the plateau has shifted from s/s_o= 0.74 to s/s_o= 0.702 for Reynolds number of 150,000. The combination of higher Reynolds number with high unsteady wakes introduce fluctuation kinetic energy into the boundary layer which tends to inhibit the separation tendency. C_p-distribution clearly shows that the wake impingement with higher Reynolds number shortens the streamwise extent of the separation zone compared to the steady case. Also, the combination of higher Re-number with unsteady wakes reveals that the noticeable deviation in pressure distribution between the steady and unsteady cases discussed above is diminishing with increasing the Re-number as shown in Figure 4(a, b). Two counteracting factors are contributing to this deviation. The first factor is attributed to the momentum deficiency and the associated total pressure losses caused by moving wakes, as discussed above. The second factor pertains

to the energizing effect of the impinging wakes on the boundary layer. Although the impinging wakes cause velocity and momentum deficits, their high turbulence intensity vortical cores provide an intensive exchange and transfer of mass, momentum, and energy to the blade surface, thus energizing the low energetic boundary layer. In conjunction with the surface pressure distribution, the kinetic energy of the normal velocity fluctuation component plays a crucial role. In case of a low Re-number flow, the strong damping effect of the wall shear stress has the tendency to reduce the normal contribution of turbulence kinetic energy, thereby diminishing its surface pressure augmenting effect. Increasing the Reynolds number results in a decrease of the damping effect of the wall shear stress, allowing the kinetic energy of the normal velocity fluctuation component to increase the surface pressure, thus offsetting the wake deficit effects on the pressure distribution. This fact is clearly shown in Figure 4(a, b), where the pressure distributions of unsteady flow cases at Ω=1.59 and Ω=3.18 systematically approach the steady state cases at Re=150,000.

Detailed information regarding the structure of the separation bubble is delivered by means of a detailed unsteady boundary layer or surface pressure measurement by fast response probes, as will be discussed in the subsequent sections.

Time Averaged Velocity Distributions

Following the surface pressure investigations that mainly addressed the onset and extent of the separation zone discussed previously, comprehensive boundary layer measurements were performed to identify the streamwise and normal extent as well as the deformation of the separation zone under unsteady wake flow. The steady state case serves as the reference configuration.

Consistent with the surface pressure distribution which is discussed above, the effect of the wake frequency on the time-averaged velocity profiles and fluctuation velocity distribution are presented for one steady and two unsteady inlet flow conditions on the suction surface along 31 streamwise locations for the Reynolds number of 110,000 and 41 streamwise locations for the Reynolds number of 150,000. After completing the velocity measurements, the boundary layer coordinates were transformed into a blade orthogonal coordinate system. Velocities at blade normal positions were obtained by interpolating their transformed values. The results showed almost no difference between the interpolated and non-interpolated velocity data. Experimental investigations were performed for three different values of Ω = 0.0, 1.59, and 3.18. These values cover the reduced frequency range encountered in LPT-design and off-design operation conditions.

The effect of wake frequency on time averaged velocity and velocity fluctuation distributions is shown in Figures 5 to 8 at 6 representative streamwise locations for Re=110,000 and Re=150,000. Upstream of the separation bubble at s/s_o= 0.52 and also at its immediate proximity s/s_o=0.588, the velocity distributions inside the boundary layer experience a slight decrease with increasing the reduced frequency. Inside the separation bubble at s/s_0=0.705, a substantial influence of the wake frequency is observed. The higher wake frequency introduces a fluctuation kinetic energy into the boundary layer trying to reverse the separation tendency. As it can be seen from the velocity distribution profiles wake impingement shortens the streamwise extent of the separation zone and decreases the bubble height, compared to the steady case, however, the onset of the separation bubble is not changed. This shows that the flow does not have the capability to suppress the separation bubble. It only reduces the separation bubble height. In the downstream of the separation bubble, where the flow is fully reattached, s/s_o=0.951, the impact of the wake on the boundary layer is reduced. This effect is clearly shown in the velocity distribution at s/s_o=0.951. According to the previous investigations by Schobeiri et al. [10] on a HP-turbine cascade, an increased wake frequency causes turbulence fluctuations to rise inside
and outside the boundary layer as shown in Figure 7 and 8. However, in the LPT case with the boundary layer separation once the boundary layer is re-attached and the velocity distribution assumes a fully turbulent profile, no major changes are observed either in the velocity or in the fluctuation velocity distribution. Although Re=150,000 shows the same phenomenon for the velocity and the fluctuation velocity distribution, it is observed that starting point of the separation bubble and the re-attachment point move further downstream to s/s_o= 0.56 and s/s_o= 0.788 respectively. Also, the size of the separation bubble is smaller when compared to that for Re=110,000.

Temporal Behavior of the Separation Zone Under Unsteady Wake Flow

Velocity distributions on the suction surface with time as the parameter are plotted in Figure 9 to 12 for Re = 110,000 and 150,000 and Ω = 1.59, 3.18. The nondimensional time (t/τ) values are chosen so that they

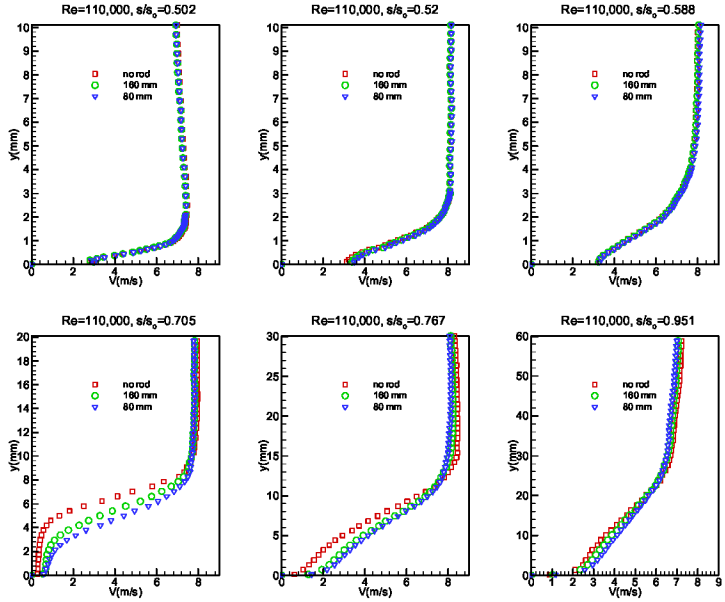

Figure 5. Distribution of time-averaged velocity along the suction surface for steady case Ω=0 (S_R=∞) and unsteady cases Ω=1.59 (S_R=160 mm) and Ω=3.18 (S_R=80 mm) at Re=110,000

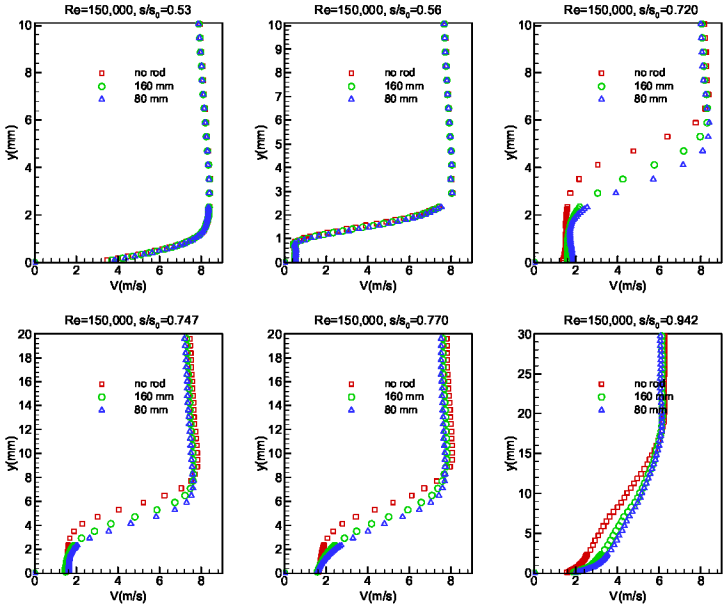

Figure 6. Distribution of time-averaged velocity along the suction surface for steady case Ω=0 (S_R=∞) and unsteady cases Ω=1.59 (S_R=160 mm) and Ω=3.18 (S_R=80 mm) at Re=150,000

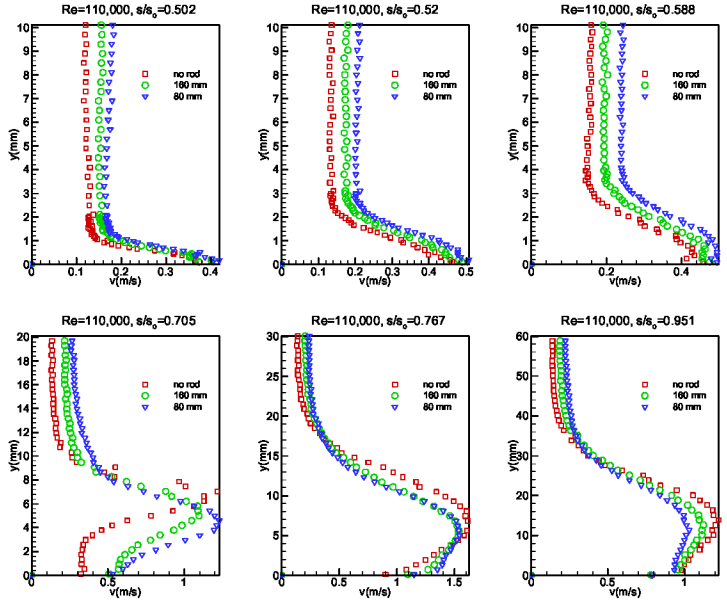

Figure 7. Distribution of time-averaged fluctuation rms velocity along the suction surface for steady case Ω=0 (S_R=∞) and unsteady cases Ω=1.59 (S_R=160 mm) and Ω=3.18 (S_R=80 mm) at Re=110,000

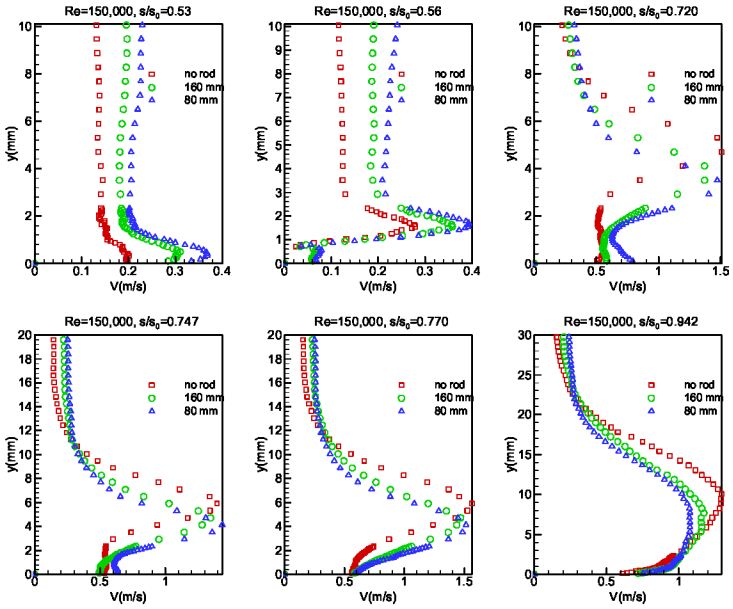

Figure 8. Distribution of time-averaged fluctuation rms velocity along the suction surface for steady case Ω=0 (S_R=∞) and unsteady cases Ω=1.59 (S_R=160 mm) and Ω=3.18 (S_R=80 mm) at Re=150,000

represent the temporal states within one full period of wake passing. For Re = 110,000 Figures 9(a) to 9(e) show, the velocity distributions inside and outside the boundary layer at fixed s/s_o- locations experience moderate to pronounced changes. Figure 9(a) represents the instantaneous velocity distribution upstream of the separation zone followed by Figures. 9(b,c,d,e) which represent the velocity distributions inside the separation zone. The last Figure 9(f) exhibits the instantaneous velocity distribution downstream of the separation zone. In discussing the following results, we simultaneously refer to the wake distribution as well as the turbulence fluctuation results.

Figure 9(a) exhibits the velocity distribution on the suction surface at $s/s_o = 0.402$. At this streamwise position, the laminar boundary layer is subjected to a strong negative pressure gradient. The boundary layer distributions at different (t/τ) experience changes in magnitude that reflect the corresponding changes of the impinging periodic wake velocity. It is worth noting, that despite the injection of turbulence kinetic energy by the impinging wakes, no local instantaneous boundary layer transition occurs. This is because of the strong negative pressure gradient that prevents the boundary layer from becoming instantaneously transitional. Instantaneous velocity distributions inside the separation zone are shown in Figures 9(b,c,d,e,f).

As a representative case, the results plotted in Figure 9(e) at $s/s_o = 0.674$ is discussed. During the time interval from t/τ close to 0.5 (1.5, 2.5, etc.) to about $t/\tau = 0.75$ (1.75, 2.75 etc.), the separation zone is exposed to the wake external flow which is under the influence of relatively lower turbulence. This flow does not have the capability to suppress the separation zone. Thus the separation region is clearly shown by the velocity distributions at $t/\tau = 0.5$ and $t/\tau = 0.75$. As the wake passes over the blade at $s/s_o = 0.674$ introducing high turbulence kinetic energy into the boundary layer, the boundary layer is energized causing the separation zone to partially reduce or disappear. This leads to an instantaneous re-attachment. This time interval corresponds to the case where the flow is completely under the influence of wake and correspondingly the reattached velocity distribution assumes a turbulent profile characterized by the curves at $t/\tau = 1.0$, $t/\tau = 0.05$, and $t/\tau = 0.25$ shown in Figure 9(e). To emphasize this statement, the steady state velocity distribution at the same streamwise position is also plotted in Figure 9(e) using full circles. It shows clearly the separated nature of the boundary layer which coincides with the instantaneous velocity profile at $t/\tau = 0.5$. Intermediate times reflect the gradual change between the separation and re-attachment as the flow is undergoing the influence of the oncoming wake. Moving to the trailing edge of the separation zone, at $s/s_o = 0.705$, Figure 9(f), a partial reduction in boundary layer thickness as the result of wake impingement is visible, however, the separation zone does not seem to disappear.

Figure 10 (a) to (f) show the velocity distributions incident outside the boundary layer at fixed s/s_o- locations experience moderate to pronounced changes at $\Omega = 3.18$. Similar instantaneous velocity distribution is observed when operating at a reduced frequency of $\Omega = 3.18$. Compared with $\Omega = 1.59$, a stronger suppression zone is noticed at $\Omega = 3.18$. When the wake passing frequency is increased over the blade, it is also increasing high turbulence kinetic energy. Therefore, boundary layer is energized comparatively more than the reduced frequency of $\Omega = 1.59$ and it causes the separation bubble partially reduce more.

As it is seen in Figure 11 and 12, increasing the Reynolds number to 150,000 causes starting point of the separation bubble and the re-attachment point move further downstream.. It is also observed that increasing the Reynolds number reduces the size of the separation bubble.

Behavior of Separation Bubble Under Wake Flow

The effect of the periodic unsteady wakes on the onset and extent of the separation bubble is shown in Figure 13 to 16 for Re=110,000 and 150,000 and for two different frequencies, namely $\Omega=1.59$ and $\Omega=3.18$. These figures display the full extent of the separation bubble and its behavior under a periodic wake flow impingement at different t/τ. The wake propagation for $\Omega=1.59$ and $\Omega=3.18$ is analyzed, and the value of t/τ corresponds to the point in the cycle at which the data acquisition system is triggered. During a rod passing period, the wake flow and the separation bubble undergo a sequence of flow states which are not noticeably different when the unsteady data are time-averaged. The temporal changes of the spatial position of the separation bubble, is compared with the time-averaged separation bubble. Starting with a reduced frequency of $\Omega=1.59$ at $t/\tau=0.25$, the separation bubble is under a full influence of the wake. The wake passing over the blade introduces a high turbulence kinetic energy into the boundary layer. The energized boundary layer bubble is partially reduced or disappeared compared to the time-averaged separation bubble size shown in Figure 13(a). As the wake passes, $t/\tau=0.50$, the height of the separation bubble reaches its maximum size at $s/s_o=0.705$. The contraction starts again that

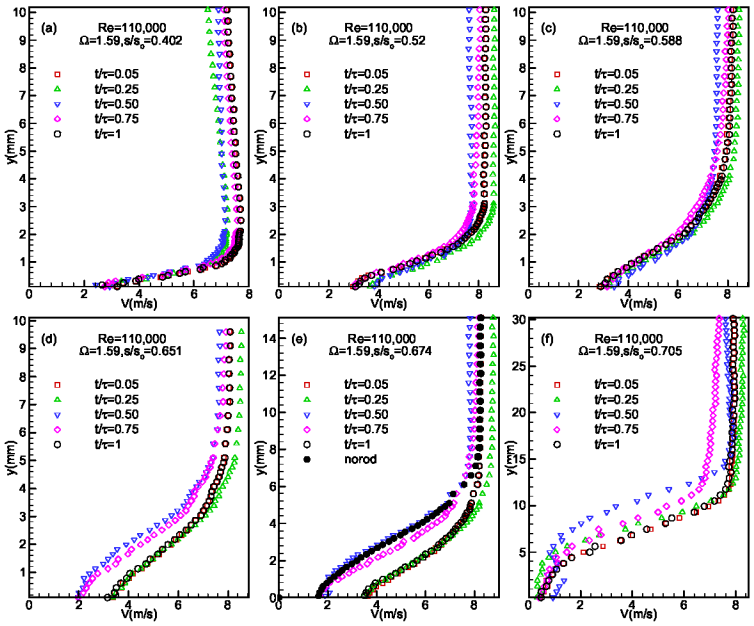

Figure 9. Distribution of the ensemble-averaged velocity development along the suction surface for different s/s_o with time t/τ as parameter for Ω=1.59 (S_R=160 mm) and Re=110,000

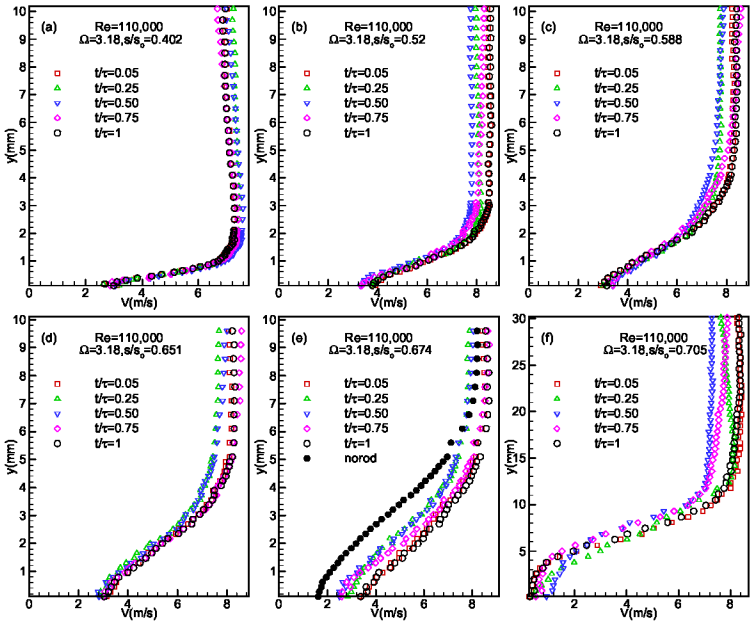

Figure 10. Distribution of the ensemble-averaged velocity development along the suction surface for different s/s_o with time t/τ as parameter for Ω=3.18 (S_R=80 mm) and Re=110,000

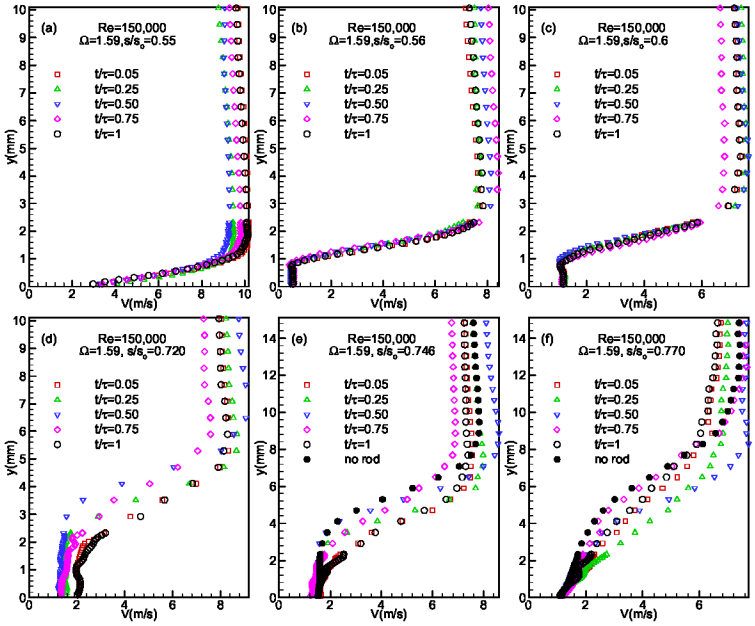

Figure 11. Distribution of the ensemble-averaged velocity development along the suction surface for different s/s_o with time t/τ as parameter for Ω=1.59 (S_R=160 mm) and Re=150,000

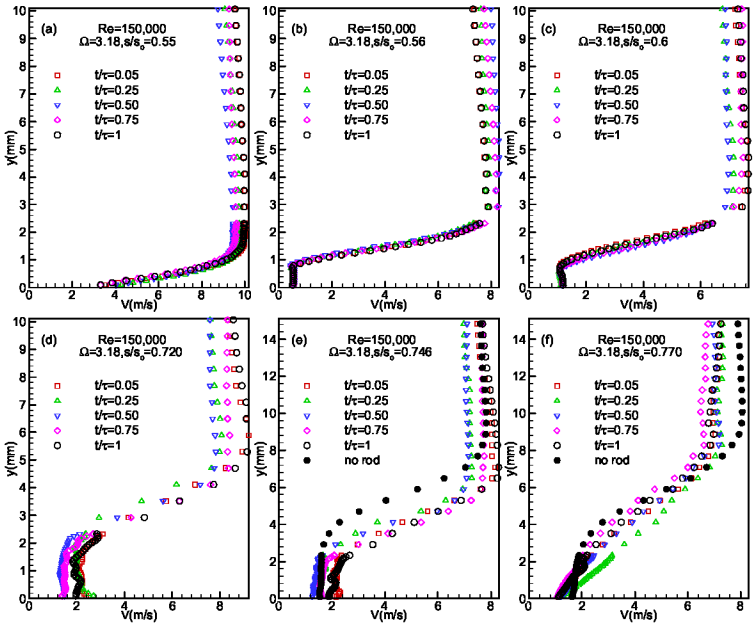

Figure 12. Distribution of the ensemble-averaged velocity development along the suction surface for different s/s_o with time t/τ as parameter for Ω=3.18 (S_R=80 mm) and Re=150,000

reduces the size of the separation bubble at $t/\tau=0.75$. At $s/s_o=0.705$ the core region has slightly moved towards to the leading edge. At $t/\tau=1$, the full effect of the wake on the boundary layer can be seen before another wake appears and the bubble moves back to the original position. Once the wake starts to penetrate into the separation bubble, the turbulent spot produced in the wake paths causes a total suppression at some streamwise positions. Similar results are observed when operating at a reduced frequency of $\Omega=3.18$ and Reynolds number of 150,000. It is observed that increasing Reynolds number to 150,000 moves the separation bubble further downstream and the wake frequency exerts no influence on the position of the separation bubble. However, doubling the reduced frequency and increasing the Reynolds number is associated with the higher turbulence intensity that leads to stronger suppression of the separation bubble as shown in Figure 14 to 16.

CONCLUSIONS

A detailed experimental study on the behavior of the separation bubble on the suction surface of a highly loaded LPT blade under periodic unsteady wake flow were investigated. The measurements were carried utilizing a custom designed hot-wire probe. One steady and two different unsteady inlet wake flow conditions with the corresponding passing frequencies, the wake velocity and the turbulence intensities were investigated by utilizing a large-scale, subsonic research facility. Translational motion of the timing belt created the unsteady wake flow. It is found that the turbulent spots generated by the unsteady wake flow were effective in suppressing or reducing the size of the separation bubble. The results of the unsteady boundary layer measurements were presented in the ensemble-averaged, and contour plot forms. Surface pressure measurements were performed at Re= 110,000 and Re=150,000. At each Reynolds number, one steady, and two periodic unsteady inlet flow measurements were performed. Slight changes of the pressure distribution occurred, while operating at the unsteady flow conditions. Increasing the Reynolds number to Re=150,000, has brought major changes in steady state C_p-distribution. The combination of higher Reynolds number with high unsteady wakes introduce fluctuation kinetic energy into the boundary layer which tends to reverse the separation tendency. C_p-distribution clearly shows that the wake impingement with higher Reynolds number shortens the streamwise extent of the separation zone compared to the steady case. Detailed unsteady boundary layer measurement identified the onset and extension of the separation bubble as well as its behavior under the unsteady wake flow. Passing the wake flow with its highly turbulent vortical core over the separation region, caused a periodic contraction and expansion of the separation bubble and a reduction of the separation bubble height. Increasing the passing frequency associated with a higher turbulence intensity further reduced the separation bubble height. It is observed that starting point of the separation bubble and the re-attachment point move further downstream to $s/s_o= 0.56$ and $s/s_o= 0.788$ respectively by increasing the Reynolds number to 150,000. Also, the size of the separation bubble is smaller when compared to that for Re=110,000.

UNCERTAINTY ANALYSIS

The Kline and McClintock [29] uncertainty analysis method was used to determine the uncertainty in the velocity after calibration and data reduction for the single-wire probe. The Kline and McClintock method determines the uncertainty with a 95% confidence level. The uncertainty in the velocity for the single-wire probe after the data reduction is given in Table 3. As shown, the uncertainty in the velocity increases as the flow velocity decreases. This is due to the pneumatic pressure transducer having a large uncertainty during calibration.

Table2: Uncertainty in velocity measurement for hot-wire probe.

$\bar{U}$ (m/s)	3	5	12
$\omega\bar{U}/\bar{U}$ $(\%)_{rcd}$	5.78	2.41	1.40

ACKNOWLEDGMENTS

The presented study is a part of an ongoing LPT-aerodynamics project executed by the NASA Glenn Research Center. The authors were supported by NASA Cooperative Agreement NCC3-793 monitored by Dr. David Ashpis. The support and the permission for publication is gratefully acknowledged. The authors also gratefully acknowledge Pratt&Whitney for providing the research community with the blade coordinates.

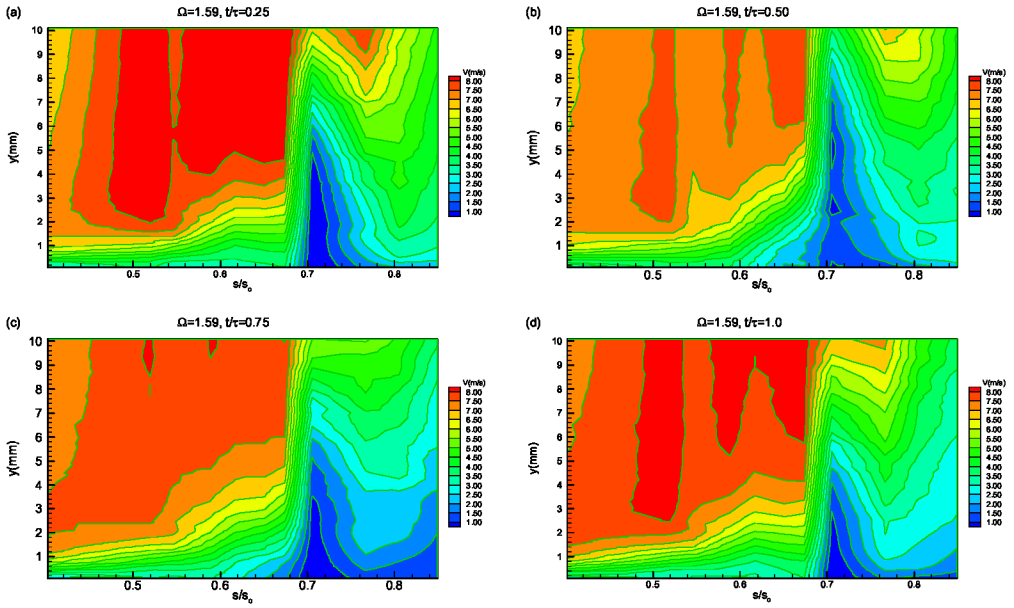

Figure 13. Ensemble-averaged velocity contours along the suction surface for different s/s_0 with time t/τ as parameter for Ω=1.59 (S_R=160 mm), Re=110,000

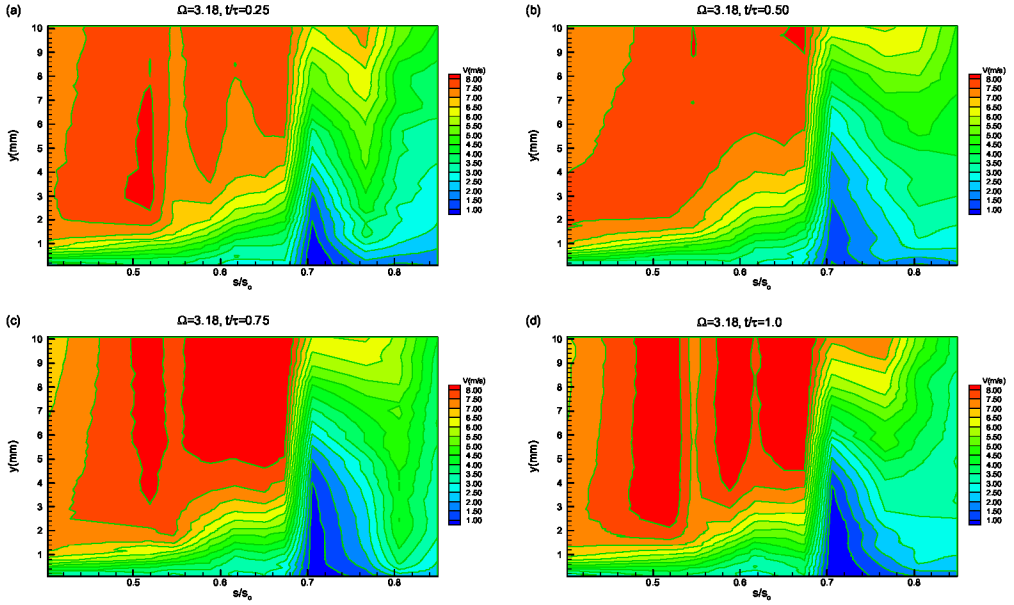

Figure 14. Ensemble-averaged velocity contours along the suction surface for different s/s_0 with time t/τ as parameter for Ω=3.18 (S_R=80 mm), Re=110,000

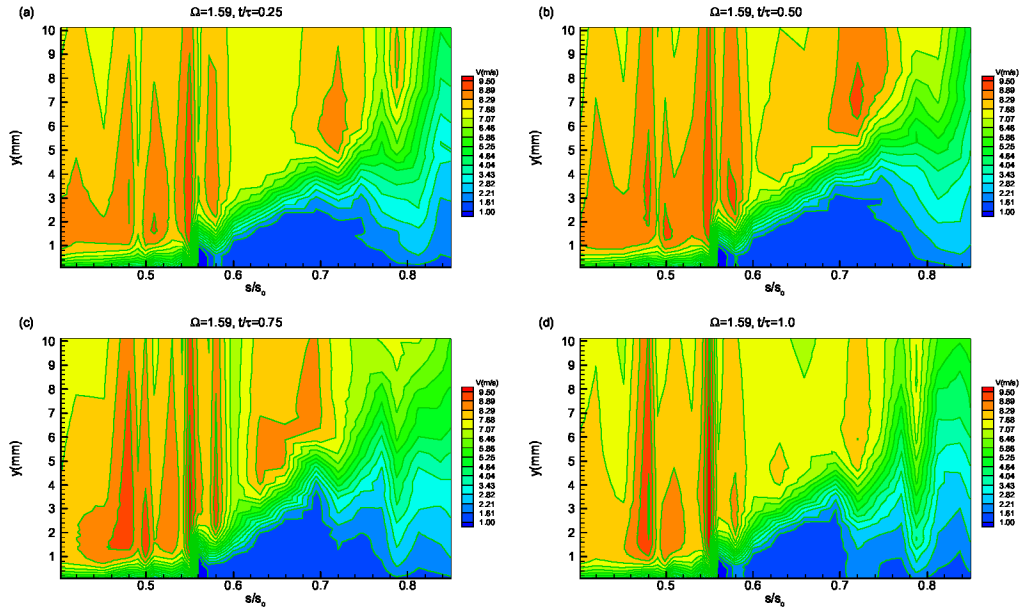

Figure 15. Ensemble-averaged velocity contours along the suction surface for different s/s_0 with time t/τ as parameter for Ω=1.59 (S_R=160 mm), Re=150,000

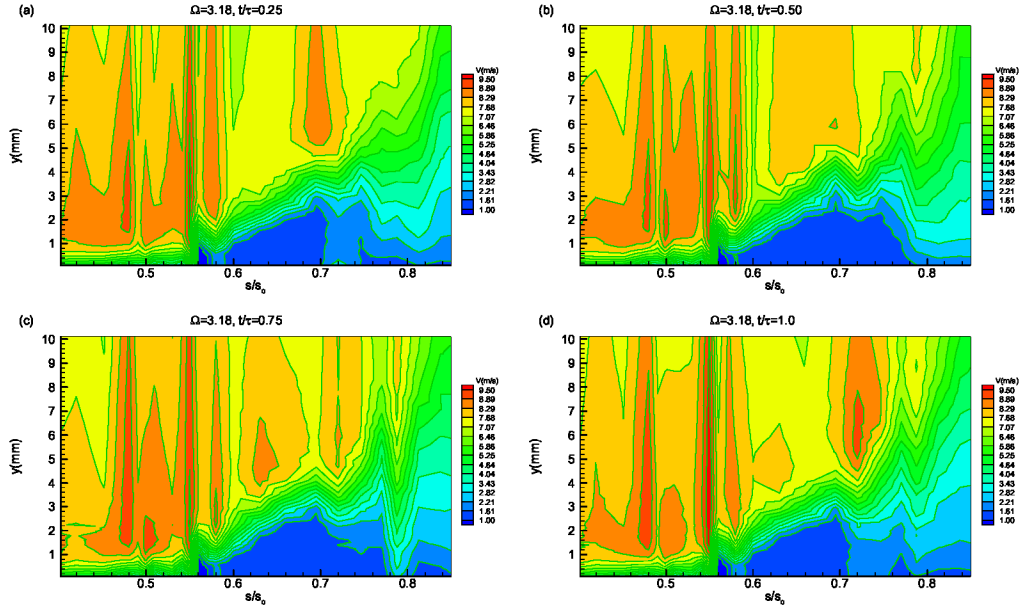

Figure 16. Ensemble-averaged velocity contours along the suction surface for different s/s_0 with time t/τ as parameter for Ω=3.18 (S_R=80 mm), Re=150,000

REFERENCES

[1] Pfeil, H., Herbst R., 1979 "Transition Procedure of Instationary Boundary Layers," ASME Paper No. 79-GT-128.

[2] Pfeil, H., Herbst, R., Schröder, T., 1983, "Investigation of the Laminar Turbulent Transition of Boundary Layers Disturbed by Wakes," ASME *Journal of Engineering for Power*, Vol. 105, pp. 130-137.

[3] Orth, U., 1993, "Unsteady Boundary Layer transition in Flow Periodically Disturbed by Wakes," ASME *Journal of Turbomachinery*, Vol. 115, pp. 707-713.

[4] Schobeiri, M. T., Radke, R. E., 1994, "Effects of Periodic Unsteady Wake Flow and Pressure Gradient on Boundary Layer Transition along the Concave Surface of a Curved Plate," ASME Paper 94-GT-327, presented at the International Gas Turbine and Aero-Engine Congress and Exposition, The Hague, Netherlands, June 13-16, 1994.

[5] Schobeiri, M.T., Read, K., Lewalle, J., 2003, "Effect of Unsteady Wake Passing Frequency on Boundary Layer Transition, Experimental Investigation and Wavelet Analysis," ASME, *Journal of Fluids Engineering*, Vol. 125. pp.251-266.

[6] Wright, L., Schobeiri, M. T., 1999, "The Effect of Periodic Unsteady Flow on Boundary Layer and Heat Transfer on a Curved Surface," ASME Transactions, *Journal of Heat Transfer*, November 1998, Vol. 120, pp. 22-33.

[7] Chakka, P., Schobeiri, M.T. , 1999, "Modeling of Unsteady Boundary Layer Transition on a Curved Plate under Periodic Unsteady Flow Condition: Aerodynamic and Heat Transfer Investigations," ASME Transactions, *Journal of Turbo machinery*, January 1999, Vol. 121, pp. 88-97.

[8] Liu, X., Rodi, W., 1991, "Experiments on Transitional Boundary Layers with Wake-Induced Unsteadiness," *Journal of Fluid Mechanics*, Vol. 231 pp. 229-256.

[9] Schobeiri, M. T., Pappu, K., Wright, L., 1995, "Experimental Sturdy of the Unsteady Boundary Layer Behavior on a Turbine Cascade," ASME 95-GT-435, presented at the International Gas Turbine and Aero-Engine Congress and Exposition, Houston, Texas, June 5-8, 1995.

[10]Schobeiri, M. T., John, J., Pappu, K., 1997, "Experimental Study on the effect of Unsteadiness on Boundary layer Development on a Linear Turbine Cascade," *Journal of Experiments in Fluids,* 23 (1997), pp. 303-316.

[11]Schobeiri, M. T., Wright, L., 2003, "Advances in Unsteady Boundary layer Transition Research," Part I and II: *International Journal of Rotating Machinery*, Volume 9 Number 1 pp, 1-22

[12] Schobeiri, M. T., Chakka, P., 2002, "Prediction of Turbine Blade Heat Transfer and Aerodynamics Using Unsteady Boundary Layer Transition Model," *International Journal of Heat and Mass Transfer*, 45 (2002) pp. 815-829.

[13]Brunner, S., Fottner, L., Schiffer, H-P., 2000, "Comparison of Two Highly Loaded Turbine Cascade under the Influence of Wake-Induced Transition," ASME 2000-GT-268, presented at the International Gas Turbine and Aero-Engine Congress and Exposition, Munich, Germany, May 8-11, 2000.

[14] Cardamone, P., Stadtmüller P., Fottner, L, Schiffer, H-P., 2000, "Numerical Investigation of the Wake-Boundary Layer Interaction on a Highly Loaded LP Turbine Cascade Blade," ASME 2002-GT-30367, presented at the International Gas Turbine and Aero-Engine Congress and Exposition, Amsterdam, Netherlands, June 3-6, 2002.

[15]Schulte, V., Hodson, H. P., 1996, "Unsteady Wake-Induced Boundary Layer Transition in High Lift LP Turbines," ASME Paper No. 96-GT-486.

[16]Kaszeta, R., Simon T.W, Ashpis, D.E., 2001,"Experimental Investigation of Transition to Turbulence as Affected by Passing Wakes ," ASME Paper 2001-GT-0195.

[17]Lou, W., Hourmouziadis, J., 2000,"Separation Bubbles under Steady and Periodic Unsteady Main Flow Conditions,"ASME Paper 200-GT-270.

[18]Volino, R. J., Hultgren L. S., 2001, "Measurements in Separated and Transitional Boundary Layers Under Low-Pressure Turbine Airfoil Conditions," ASME, *Journal of Turbomachinery*, Vol. 123, pp. 189-197.

[19]Schröder, Th., 1989, "Measurements with Hot-Film Probes and Surface Mounted Hot Film Gages in a Multi-Stage Low Pressure Turbine," European Propulsion Forum, Bath, UK.

[20]Haueisen V., Hennecke D.K., Schröder, T., 1997, "Measurements With Surface Mounted Hot Film Sensors on Boundary Layer Transition in Wake Disturbed Flow," AGARD-CP-598.

[21]Shyne, R. J., Sohn K. H., De Witt, K. J., 2000, " Experimental Investigation of Boundary Layer Behavior in a Simulated Low Pressure Turbine," ASME, *Journal of Fluids Engineering*, Vol. 122, pp. 84-89.

[22]Treuren, K. W. V., Simon T., Koller M. V., Byerley A. R., Baughn J. W., Rivir, R., 2002, " Measurements in a Turbine Cascade Flow under Ultra Low Reynolds Number Conditions," ASME, *Journal of Turbomachinery*, Vol. 124, pp. 100-106.

[23]Halstead, D.E., Wisler, D, C., Okiishi, T.H, Walker, G.J., Hodson, H.P., and Shin, H.-W, ,1997, "Boundary Layer Development in Axial Compressors and Turbines: Part 3 of 4," ASME *Journal of Turbomachinery*, 119, pp. 225-237.

[24]Schobeiri, M. T., Öztürk, B., 2003, " On the Physics of the Flow Separation Along a Low Pressure Turbine Blade Under Unsteady Flow Conditions,"ASME 2003-GT-38917, presented at International Gas Turbine and Aero-Engine Congress and Exposition, Atlanta, Georgia, June 16-19, 2003.

[25]Schobeiri, M. T., Öztürk, B., 2003, " Experimental Study of the Effect of the Periodic Unsteady Wake Flow on Boundary Layer development, Separation, and Re-attachment Along the Surface of a Low Pressure Turbine Blade,"ASME 2004-GT-53929, presented at International Gas Turbine and Aero-Engine Congress and Exposition, Vienna, Austria, June 14-17, 2004.

[26]Schobeiri, M. T., John, J., Pappu, K., 1996, "Development of Two-Dimensional Wakes Within Curved Channels, Theoretical Framework and Experimental Investigation," ASME Transactions, *Journal of Turbomachinery*, July, 1996, Vol. 118, pp. 506-518.

[27]Hourmouziadis, J., 1989, "Blading Design for Axial Turbomachines," AGARD, Lecture Series LS-167.

[28]Eifler, J., 1975, "Zur Frage der freien turbulenten Strömungen, insbesondere hinter ruhenden und bewegten Zylindern," Dissertation D-17, Technische Hochschule Darmstadt, Germany.

[29]Kline, S. J., McKlintock, F.A., "Describing Uncertainties in Single-Sample Experiments," *Mechanical Engineering*, Vol. 75, Jan. 1953, pp. 38.